An analysis of the axisymmetric three-dimensional low level wind field in a tornado using mobile radar observations

Karen A. Kosiba,[1] and Robert J. Trapp,[1] and Joshua Wurman[2]

Received 28 August 2007; revised 4 January 2008; accepted 30 January 2008; published 6 March 2008.

[1] The purpose of this letter is to present an analysis of the three-dimensional wind field retrieved from mobile Doppler radar data of the 12 May 2004 Harper, KS tornadoes. The derived three-dimensional vortex structure and its surrounding flow show marked temporal and spatial variability. This has significant implications on the numerical modeling of tornado-scale flow. **Citation:** Kosiba, K. A., R. J. Trapp, and J. Wurman (2008), An analysis of the axisymmetric three-dimensional low level wind field in a tornado using mobile radar observations, *Geophys. Res. Lett.*, *35*, L05805, doi:10.1029/2007GL031851.

1. Introduction

[2] Although theory, modeling, and observations have provided us with a general framework for understanding tornadic flow, obtaining a comprehensive picture of the low-level wind field remains an ongoing endeavor. The near-surface winds are a complex interaction of three dynamically different regions of flow: the swirling boundary layer, the corner region and the core flow (e.g., see the review by *Davies-Jones et al.* [2001]). A simplified view of the interaction between these regions consists of the boundary layer feeding the vortex core by way of the corner region. The boundary layer, which is believed to comprise roughly the lowest tens of meters of the flow, forms as a result of the strong interaction of the primary rotating flow with the underlying surface. Above the boundary layer, the flow is thought to approximate cyclostrophic balance and dictates the magnitude of the radial pressure gradient force in the boundary layer. Since frictional interaction necessarily reduces the tangential velocity to zero at the surface, an imbalance is created between the centrifugal and radial pressure gradient forces. This imbalance drives a net inward acceleration, resulting in increased tangential velocities in the mid- to upper-boundary layer.

[3] Flow diverted into the boundary layer and subsequently into the core must pass through the corner region, the most dynamically complex region of the tornado. Unlike in other regions of the tornado, all three components of velocity are important. The corner region has approximately the same vertical extent as the boundary layer and the same horizontal extent as the core and is where the horizontal boundary layer flow must turn vertical. Flow in this region can be additionally complicated by the presence of vortex breakdown (the rotational analog of a hydraulic jump), which can result in the largest velocities occurring very close to the ground. Since the vortex core consists of air that has entered either from the flow aloft or from the boundary layer, changes in the boundary layer flow can substantially alter the core by way of the corner region. Indeed, *Lewellen et al.* [2000] have underscored the importance of low-level angular momentum flux to the near-surface vortex intensification process. They demonstrate that near-surface vortex intensity is decreased as the inward flux of low-level angular momentum from the immediate environment of the tornado (i.e., the outer core region) is depleted. The important implication here is that a characterization of the low-level angular momentum distribution in the outer core could potentially provide needed information about the corner flow and tornado core dynamics.

[4] The objective of this letter is to characterize the three-dimensional outer flow field of one of the 12 May 2004 Harper County, KS tornadoes and its subsequent relationship to vortex structure. This is accomplished with the aid of mobile Doppler radar technology, which has been particularly successful in providing high-resolution, near-surface observations of tornadoes [e.g., *Bluestein and Pazmany*, 1999; *Lee and Wurman*, 2005; *Wurman and Gill*, 2000; *Wurman and Alexander*, 2005]. Although radar observations are of (scatterer) motion parallel to the radar beam, the characteristic three-dimensional wind field can be retrieved from volume scans by making some *a priori* assumptions about the nature of the flow.

2. Methodology

[5] In order to retrieve the radial (u), tangential (v), and vertical (w) winds from the measured Doppler velocities (V_D), we have elected to apply the approach described by *Dowell et al.* [2005], which in effect is a simplified version of the ground-based Velocity Track Display (GBVTD) technique devised by *Lee et al.* [1999]. Underlying the *Dowell et al.* approach is the critical assumption that the tornado and its surrounding flow can be considered a superposition of axisymmetric rotational and divergent flows in conjunction with the translational velocity of the tornado. Consequently, we are only retrieving the axisymmetric, or wavenumber 0, component of the flow. Although there is some evidence in the data of wavenumber 2 asymmetries in the core flow, the surrounding flow (i.e., the outer core flow) appears to be to be primarily axisymmetric.

[6] For a given radar volume scan, the observed (quasi-horizontal) Doppler velocity (V_D) can then be expressed as follows:

$$V_D = u\cos(\alpha - \theta) + v\sin(\alpha - \theta) + C\cos(\beta - \theta) \qquad (1)$$

[1]Department of Earth and Atmospheric Sciences, Purdue University, West Lafayette, Indiana, USA.
[2]Center for Severe Weather Research, Boulder, Colorado, USA.

0094-8276/08/2007GL031851$05.00

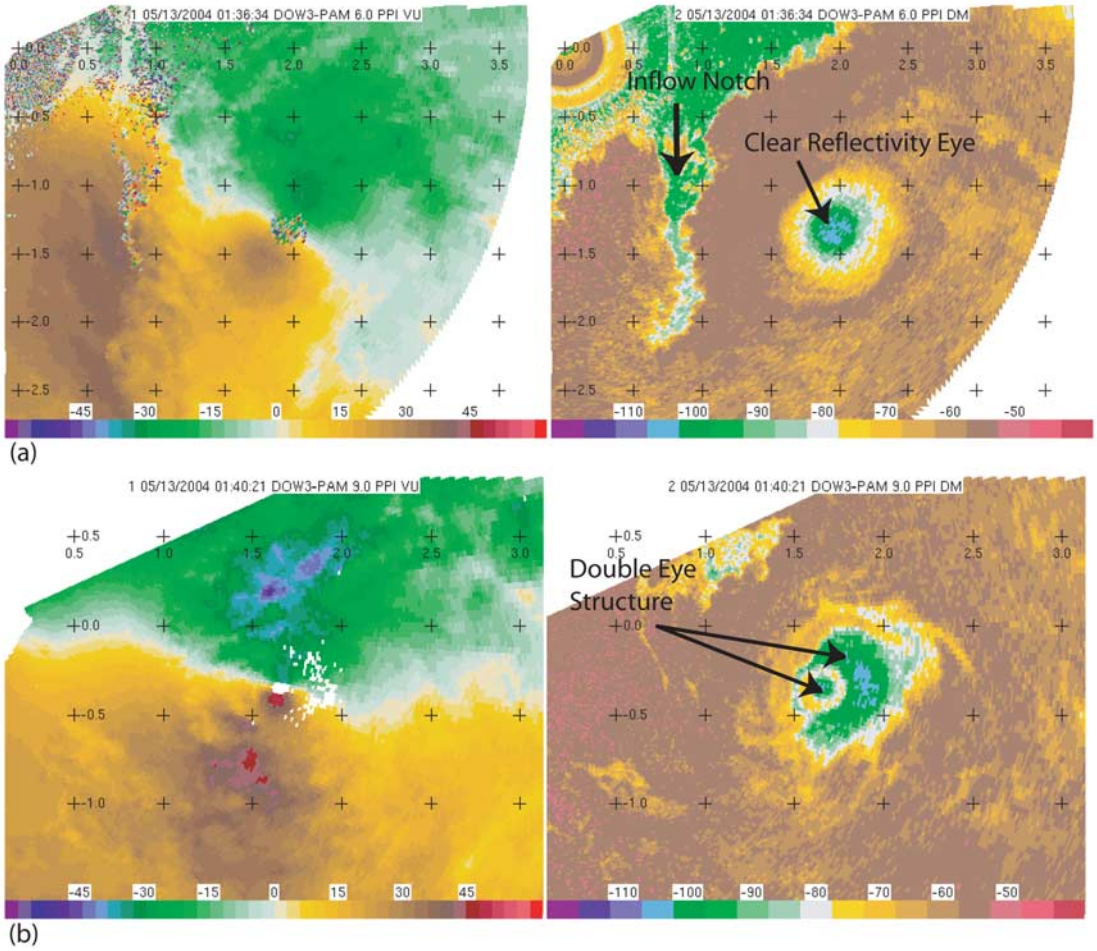

Figure 1. Examples of the salient features observed in the Harper, KS tornado in which (a) the inflow notch and the clear eye are observed and (b) the double eye structure is observed. In both Figure 1a and Figure 1b, the image on the left is Doppler velocity and the image on the right is radar reflectivity.

where α is the angle of the observation with respect to the tornado center, θ is the angle of the observation with respect to the radar, and C and β quantify the constant flow within which the tornado vortex is embedded. Here, C is comprised of the low-level environmental wind and the tornado/storm motion, which appear to be nearly equivalent in this case, and β is the flow angle with respect to the tornado center. In this formulation, the vertical wind component (and terms involving elevation angle) is omitted because the scans are at low elevation angles. Note that when the *Lee et al.* [1999] formulation is truncated at wavenumber 0, equation (1) is equivalent to the GBVTD equation.

[7] Solving equation (1) in a least squares sense in an annulus surrounding the vortex center yields the following relations for the azimuthally-averaged (wavenumber 0) radial and tangential winds:

$$u(r) = \frac{\sum_i a_i^2 \sum_i b_i c_i - \sum_i a_i b_i \sum_i a_i c_i}{\sum_i a_i^2 \sum_i b_i^2 - \left(\sum_i a_i b_i\right)^2}$$
$$v(r) = \frac{\sum_i b_i^2 \sum_i a_i c_i - \sum_i a_i b_i \sum_i b_i c_i}{\sum_i a_i^2 \sum_i b_i^2 - \left(\sum_i a_i b_i\right)^2} \quad (2)$$

where i refers to the index of the observation along the annulus and $a_i = \sin(\alpha_i - \theta_i)$, $b_i = \cos(\alpha_i - \theta_i)$, and $c_i = V_{Di} - C\cos(\beta_i - \theta_i)$. Testing of this retrieval technique on an axisymmetric analytical velocity field [*Brown and Wood*, 1991, see their appendix B], revealed errors of less than 10% for both the retrieved tangential and the radial axisymmetric velocities.

[8] Equation (2) is closed by estimating C and β from the tornado motion. This motion was determined in the radar data by tracking the center of the tornado at the 100 m level between successive volume scans. Each location, then, has a different C and β to be incorporated into the wind retrievals. At each analysis level, the center of the tornado was defined as the midpoint between the maximum inbound and outbound Doppler velocities [*Wood and Brown*, 1992]. If needed, the location of the midpoint was adjusted based on visual inspection of the data.

[9] The assumption of axisymmetry allows for the horizontal (h) divergence to be calculated from the radial wind component: $\nabla_h \cdot \vec{V} = \frac{\partial u}{\partial r} + \frac{u}{r}$. Once the axisymmetric horizontal divergence is found, the continuity equation is integrated to obtain the axisymmetric vertical wind (w): $\rho w = -\int_{z(k)}^{z(k+1)} \rho(\nabla_h \cdot \vec{V})dz$. Two other pertinent quantities used

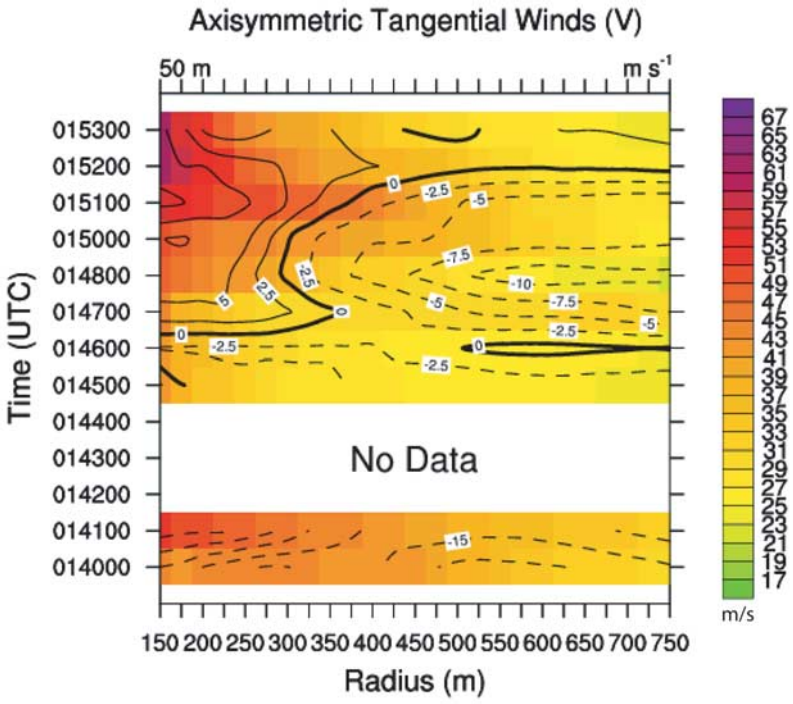

Figure 2. Axisymmetric radial and tangential winds of the Harper, KS tornado as a function of time. Both horizontal wind components are shown at 50 meters above ground level. The line contours depict the radial winds and the color contours depict the tangential winds.

to diagnose the kinematics of the tornado and of the surrounding flow, vertical vorticity (ζ) and the angular momentum (M), are derived from the retrieved winds: $\zeta = \frac{\partial v}{\partial r} + \frac{v}{r}$ and $M = vr$.

3. Description of the Data

[10] The Doppler on Wheels (DOW) [*Wurman et al.*, 1997] collected data on several tornadoes that occurred in Harper County, KS on 12 May 2004. During this event, a few structures incurred varying degrees of damage, resulting in Fujita-Scale (F-Scale) ratings for the eleven tornadoes between F0 and F4. Between 0140:45 and 0154:39 UTC (all times hereinafter are given in UTC), many salient tornado features are observed in the radar data (Figure 1) such as an inflow notch, a clear eye, and a double eye structure [e.g., *Wurman et al.*, 1996; *Bluestein and Pazmany*, 1999; *Wurman and Gill*, 2000]; consequently the diagnosed kinematics are particularly pertinent. As such, the aforementioned interval was the focus of our analysis.

[11] Fortunately, the DOW was proximal to the tornado during the prescribed time interval, sampling it at ranges of approximately 1.5 km to 3.5 km. Gate spacing (i.e., the range resolution) varies from 12.5 m, in earlier observations, to 25 m, in later observations. Quasi-horizontal sector scans exist from very near the surface ($\sim$15–30 m above ground level, AGL) upwards to several hundred meters AGL (volume scans were completed approximately every 50 seconds, thus corresponding to the temporal resolution for a given elevation). Due to the necessary time evolution between subsequent elevation angles, lower level data and upper level data do not necessarily correspond to the same dynamical manifestation of the tornado.

[12] Post-processing of the data was done before the axisymmetric retrieval technique was applied. Ground clutter was interactively removed from the data using the NCAR SOLOII software [*Oye et al.*, 1995]. The lowest elevation scans were often significantly contaminated by ground clutter in the vicinity of the tornado, necessitating the removal of large portions of data. However, the overall structure beyond the radius of maximum winds was preserved. The data were then bilinearly interpolated to a Cartesian coordinate grid with a gridpoint spacing of 25 m; this was chosen to accommodate the varied azimuthal and range resolution of the data.

[13] Tornadogenesis ensued before the analysis period and by 0135:55 a weak tornado (ΔV_D = 75 m/s, the difference between peak inbound and outbound velocities in the tornado couplet), exhibiting a low reflectivity eye, is well defined in the lowest elevation scan. Between 0135:55 and 0142:42, the tornado continues to strengthen and by 0141:58, the ground relative Doppler velocities associated with the tornado are of F3 intensity (V_D > 75 m/s). Interestingly, at 0140:04 evidence of the double eye structure (Figure 1b) emerges in both the velocity and reflectivity fields. By the next volume scan, though, this feature is no longer present. Full volume scans were unavailable during the subsequent two minutes; consequently no analysis was conducted during this interval. In the volume scan immediately following this data gap, the tornado shrinks in size and diminishes in intensity. Subsequently the tornado intensifies and by 0153:42 it reaches its peak Doppler velocity (V_D) of 94 m/s, which occurs at approximately

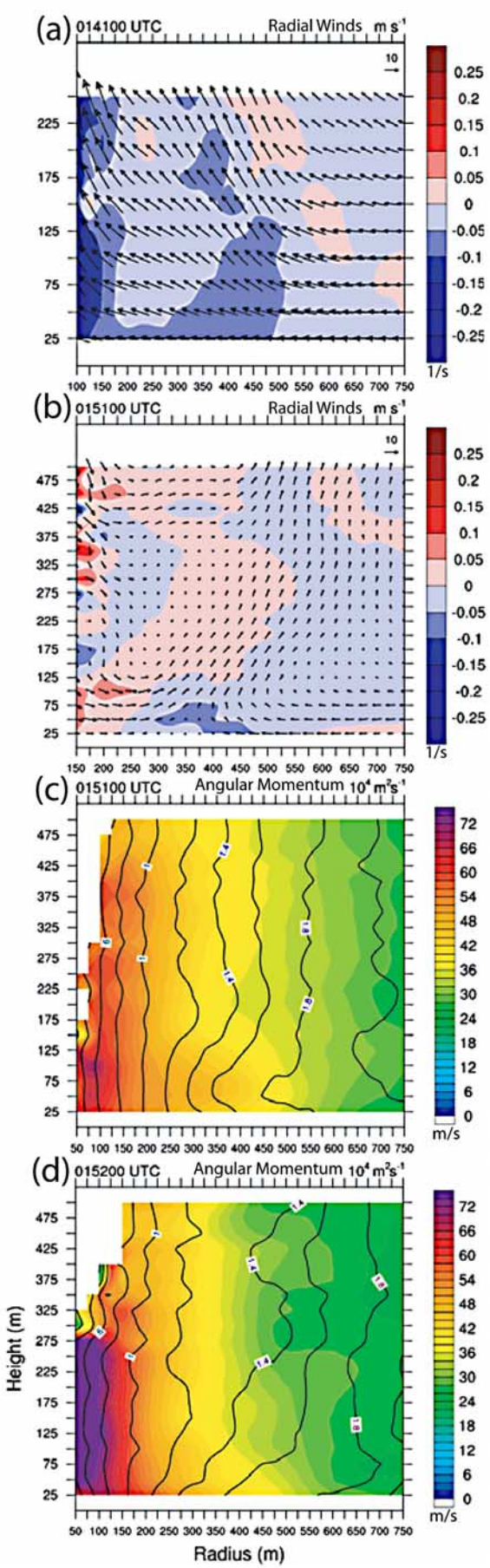

Figure 3. Axisymmetric structure (radius-height) of the Harper, KS tornado. The secondary circulation (vectors) and divergence (colored contours) are shown at (a) 0141:00 UTC and (b) 0151:00 UTC. The axisymmetric tangential winds (colored contours) and angular momentum (line contours) are shown at (c) 0151:00 UTC and (d) 0152:00 UTC.

40 m AGL. After 0156, the tornado of interest dissipates to the north while another tornado forms to the west of the radar.

[14] There are a couple of caveats to this analysis that merit discussion. When the double eye structure is present, the smaller (radius) velocity couplet was excluded from the analysis. Consequently, the center of the tornado was taken to be the midpoint of the larger (radius) velocity couplet. It is also important to note that retrievals within the radius of maximum winds, most notably at later times, should be viewed with caution as a lack of scatterers and few data are characteristic of this region. Data outside of the radius of maximum winds, effectively the outer core region, do not suffer from such restrictions and are thus thought to give an accurate depiction of the outer flow regime. This is particularly significant for future modeling studies that make use of the outer flow conditions as lateral boundary conditions on a tornado vortex model.

4. Retrieved Three-Dimensional Winds

[15] Figure 2 depicts the evolution of the axisymmetric horizontal winds of the tornado at 50 m AGL. Initially, there is strong flow (~20 m/s) into the tornado at all radii. The initial surge of inflow is accompanied by a comparatively large swath of tangential winds in excess of 32 m/s (the lower bound on F0 winds). After 0141:00 (all times are referenced to the minute corresponding to the start of the volume scan), the tornado contracts, as is evidenced by the decrease in the radius of maximum winds (RMW). After this contraction, the tornado increases in both size and intensity (as measured by the peak tangential winds) so that between 0150:00 and 0153:00, the tornado was not only at peak intensity, but additionally winds in excess of 32 m/s extended well beyond the RMW. Further, as the tornado evolves, the flow within approximately the RMW becomes noticeably divergent (denoted by the thick black line in Figure 2).

[16] It is pertinent to compare this velocity evolution (Figure 2) to the inferred change in vortex structure (Figures 3a and 3b). Earlier retrievals indicate a much different vortex structure than at later times. Figure 3 depicts the radial winds as a function of height and radius at 0141:00 (Figure 3a) and 0151:00 (Figure 3b). At 0141:00, strong inflow not only exists at all radii, but it also extends through the depth (250 m) of the analysis domain. Correspondingly, the flow is predominantly convergent and exhibits a one-celled structure. Ten minutes later, at 0151:00, a markedly different vortex structure emerges. Flow within the RMW is now divergent, whereas flow outside of the RMW is still convergent. This change in the radial velocity within the RMW may be indicative of the transition to a two-celled vortex, which is elucidated by the development of a downdraft near the central axis (Figure 3b). As exemplified in

Table 1. Best Fit Decay Coefficient α in the Modified Rankine Vortex as a Function of Time

Time, UTC	0140	0145	0146	0147	0151	0152	0153
α	0.26	0.46	0.47	0.45	0.43	0.56	0.61

Figure 3b, a relatively shallow inflow layer ($\sim$100 m) still exists in the lowest portion of the domain.

[17] Figure 3d depicts the angular momentum at 0152:00, when the tornado is most intense. Of interest is the low-level angular momentum at larger radii. One can infer from Figure 3d that higher angular momentum air is being imparted to the vortex at lower levels. In the context of a local swirl ratio [*Lewellen et al.*, 2000], this transport of higher low-level angular momentum into the vortex should lead to an increase in the local swirl ratio and, consequently, a more intense low level vortex. Indeed within this volume the largest velocities are observed, but the low level angular momentum distribution in the prior volume (Figure 3c) suggests that low level angular momentum is being depleted in the lower portion of the analysis domain. Several possibilities exist that could explain this discrepancy. For example, the relevant angular momentum distribution may lie below the lowest observation level. Or, consistent with the intensity evolution of the tornado, the angular momentum transport is progressively downward and inward. Finally, it is also possible that ground clutter may have contaminated the low level data.

[18] It is also worthwhile to note that within approximately the RMW, the angular momentum is relatively constant with height (Figures 3c and 3d). This characteristic profile is ubiquitous throughout the observational period. The Mulhall tornado [*Lee and Wurman*, 2005, Figure 4h] exhibited a similar angular momentum distribution. Analysis of the axisymmetric angular momentum associated with hurricanes [e.g., *Lee et al.*, 2000] reveals a similar distribution, suggesting that such a profile is endemic of intense vortices.

[19] Further insight into the relevant vortex dynamics is obtained by comparing the axisymmetric tangential wind profiles to those of a modified Rankine vortex ($V = R^{-\alpha}$). The tangential velocities were normalized and the outer flow (i.e., the potential vortex) attributes were examined. Averaging these profiles through the volume and relating them via the relationship described by *Mallen et al.* [2005] yielded characteristic decay coefficients (α) for each volume scan. As a decay coefficient of 1 would indicate a potential vortex (i.e., angular momentum would be conserved as it spirals in), decay coefficients less than 1 indicate a loss of fluid momentum. Examining Table 1, α values were smaller at earlier times than at later times. This may indicate that more angular momentum was being depleted throughout the analysis domain in earlier observations than in later observations. Correspondingly, a vortex of lower intensity (i.e., lower tangential winds) was present in the earlier observations. Again, the values obtained for α are characteristic of other tornadoes and strong hurricanes [*Wurman and Gill*, 2000; *Wurman and Alexander*, 2005; *Lee and Wurman*, 2005; *Mallen et al.*, 2005].

[20] Examining the evolution of the vertical distribution of the axisymmetric horizontal velocities at 700 m from the center of the tornado (a reasonable proxy for the boundary of a tornado-scale model), it is evident that there are significant temporal and spatial fluctuations (Figure 4). Looking first at the radial winds (Figure 4a), a jet is present at all times except in two of the observations. As the height of the radial jet fluctuates in time, the lack of a radial jet in the earliest analysis appears to be a consequence of the height of the lowest observations. Since, at these times, the maximum radial velocity occurs at the lowest observation level, it is relatively straightforward to infer that the radial jet occurs below this level. The tangential velocities at 700 meters (Figure 4b) are quite a bit more variable than the radial velocities. A logarithmic profile typical of a turbulent boundary layer has been superimposed for comparison. One can easily see that all of the tangential velocities deviate from this idealized distribution.

5. Discussion and Implications

[21] Changes in the outer core region of a tornado can affect the properties of the flow diverted into the boundary layer, and thus the overall structure and evolution of a tornado's velocity field. Through analysis of mobile radar observations, this study has shown that the outer core region displays significant spatial and temporal variability. This has

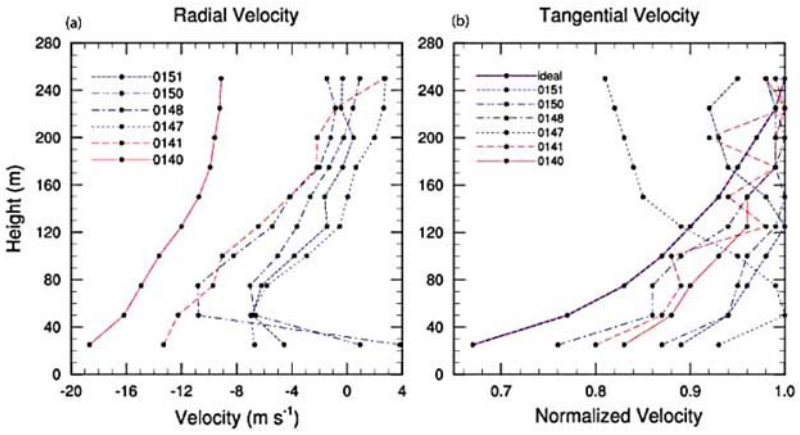

Figure 4. Axisymmetric (a) radial and (b) tangential winds at a radius of 700 meters. The tangential winds have been normalized in order to make a comparison with an idealized logarithmic profile (purple line).

ramifications for the numerical modeling of tornado-scale flow, because such simulations depend upon the boundary conditions to relay the relevant outer flow dynamics to the interior of the model domain.

[22] As discussed earlier, the vortex structure and velocities are markedly different during the prescribed analysis interval. To the extent that variations in the outer flow affect the core region remains unknown. This relationship will be investigated in a future modeling study.

[23] **Acknowledgments.** We would like to thank the ROTATE 2004 participants for their assistance during the field experiment. Curtis Alexander, Herbert Stein, and Joshua Wurman crewed DOW3 during the tornado intercept.

References

Bluestein, H. B., and A. L. Pazmany (1999), Observations of tornadoes and other convective phenomena with a mobile, 3-mm wavelength Doppler radar: The spring 1999 field experiment, *Bull. Am. Meteorol. Soc.*, *81*, 2939–2951.

Brown, R. A., and W. T. Wood (1991), On the interpretation of single-Doppler velocity patterns within severe thunderstorms, *Weather Forecasting*, *6*, 32–48.

Davies-Jones, R. P., R. J. Trapp, and H. B. Bluestein (2001), Tornadoes and tornadic storms, in *Severe Convective Storms*, *Meteorol. Monogr.*, vol. 50, pp. 167–222, Am. Meteorol. Soc., Boston, Mass.

Dowell, D. C., C. R. Alexander, J. M. Wurman, and L. J. Wicker (2005), Centrifuging of hydrometeors and debris in tornadoes: Radar-reflectivity patterns and wind-measurement errors, *Mon. Weather Rev.*, *133*, 1501–1524.

Lee, W.-C., and J. Wurman (2005), Diagnosed three-dimensional axisymmetric structure of the Mulhall tornado on 3 May 1999, *J. Atmos. Sci.*, *62*, 2373–2393.

Lee, W.-C., J.-D. Jou, P.-L. Chang, and S.-M. Deng (1999), Tropical cyclone kinematic structure retrieved from single Doppler observations. part I: Interpretation of Doppler velocity patterns and the GBVTD technique, *Mon. Weather Rev.*, *127*, 2419–2439.

Lee, W.-C., J.-D. Jou, P.-L. Chang, and F. D. Marks (2000), Tropical cyclone kinematic structure retrieved from single-Doppler radar observations. part III: Evolution and structure of Typhoon Alex, 1987, *Mon. Weather Rev.*, *128*, 3982–4001.

Lewellen, D. C., W. S. Lewellen, and J. Xia (2000), The influence of a local swirl ratio on tornado intensification near the surface, *J. Atmos. Sci.*, *57*, 527–544.

Mallen, K. J., M. T. Montgomery, and B. Wang (2005), Reexamining the near-core radial structure of the tropical cyclone primary circulation: Implications for vortex resiliency, *J. Atmos. Sci.*, *62*, 408–425.

Oye, R., C. Mueller, and S. Smith (1995), Software for radar data translation, visualization, editing, and interpolation, paper presented at 27th Conference on Radar Meteorology, Am. Meteorol. Soc., Vail, Colo.

Wood, V. T., and R. A. Brown (1992), Effects of radar proximity on single-Doppler velocity signatures of axisymmetric rotation and divergence, *Mon. Weather Rev.*, *120*, 2798–2807.

Wurman, J., and C. R. Alexander (2005), The 30 May 1998 Spencer, South Dakota, storm. Part II: Comparison of damage and radar-derived winds in the tornadoes, *Mon. Weather Rev.*, *113*, 97–119.

Wurman, J., and S. Gill (2000), Fine-scale radar observations of the Dimmitt, Texas (2 June 1995), tornado, *Mon. Weather Rev.*, *128*, 2135–2163.

Wurman, J., J. Straka, and E. Rasmussen (1996), Fine-scale Doppler radar observations of tornadoes, *Science*, *21*, 1774–1777.

Wurman, J., J. Straka, E. Rasmussen, M. Randall, and A. Zahari (1997), Design and deployment of a portable, pencil-beam, pulsed, 3-cm Doppler radar, *J. Atmos. Oceanic Technol.*, *14*, 1502–1512.

K. A. Kosiba and R. J. Trapp, Department of Earth and Atmospheric Sciences, Purdue University, 550 Stadium Mall Drive, West Lafayette, IN 47907, USA. (kakosiba@purdue.edu)

J. Wurman, Center for Severe Weather Research, 1945 Vassar Circle, Boulder, CO 80305, USA.